

# **USING GNSS TO EVALUATE THREATS TO THE MOBILITY OF RESOURCES AND PEOPLE ON COASTAL ROADS IN USDOT REGION 10**

## **FINAL PROJECT REPORT**

by

Meagan Wengrove and Jijye Park  
Oregon State University

Sponsorship  
PacTrans  
Oregon State University

for

Pacific Northwest Transportation Consortium (PacTrans)  
USDOT University Transportation Center for Federal Region 10  
University of Washington  
More Hall 112, Box 352700  
Seattle, WA 98195-2700

In cooperation with U.S. Department of Transportation,  
Office of the Assistant Secretary for Research and Technology (OST-R)



## **DISCLAIMER**

The contents of this report reflect the views of the authors, who are responsible for the facts and the accuracy of the information presented herein. This document is disseminated under the sponsorship of the U.S. Department of Transportation's University Transportation Centers Program, in the interest of information exchange. The Pacific Northwest Transportation Consortium, the U.S. Government and matching sponsor assume no liability for the contents or use thereof.

**TECHNICAL REPORT DOCUMENTATION PAGE**

<b>1. Report No.</b>		<b>2. Government Accession No.</b> 01723939		<b>3. Recipient's Catalog No.</b>	
<b>4. Title and Subtitle</b> Using GNSS to Evaluate Threats to the Mobility of Resources and People on Coastal Roads in USDOT Region 10				<b>5. Report Date</b> 29 Nov 2021	
				<b>6. Performing Organization Code</b>	
<b>7. Author(s) and Affiliations</b> Meagan Wengrove, 0000-0001-7391-8574; School of Civil and Construction Engineering, Oregon State University Jihye Park, School of Civil and Construction Engineering, Oregon State University				<b>8. Performing Organization Report No.</b> 2019-S-OSU-3	
<b>9. Performing Organization Name and Address</b> Pacific Northwest Transportation Consortium University Transportation Center for Federal Region 10 University of Washington More Hall 112 Seattle, WA 98195-2700				<b>10. Work Unit No. (TRAIS)</b>	
				<b>11. Contract or Grant No.</b> 69A3551747110	
<b>12. Sponsoring Organization Name and Address</b> United States Department of Transportation Research and Innovative Technology Administration 1200 New Jersey Avenue, SE Washington, DC 20590				<b>13. Type of Report and Period Covered</b> Final Report, June 2019-Nov. 2021	
				<b>14. Sponsoring Agency Code</b>	
<b>15. Supplementary Notes</b> Report uploaded to: <a href="http://www.pactrans.org">www.pactrans.org</a>					
<b>16. Abstract</b> USDOT Region 10 includes three states that have extensive lengths of coastal roads (Oregon, Washington, and Alaska). In each state, long stretches of oceanfront roads are the only way to move goods and people between coastal cities and inland population centers, which makes their potential vulnerability critical. In each of Oregon, Washington, and Alaska, coastal erosion due to high water levels and high waves is a known hazard. Roads perched on top of coastal bluffs are at risk because of undercutting from combined high water levels and waves (Olsen et al. 2009), and roads near sea level on open coasts are at risk because of changing shorelines. Our objective was to develop a new technique to assess the hazard level of coastal erosion hotspots on existing and planned coastal roadways by continuously monitoring coastal water levels and wave heights with a new remote sensing technique the incorporates the land-based Global Navigation Satellite System (GNSS). The proposed technique measures nearshore water levels and wave heights using land-based and easily mobilized GNSS, which is an all-weather, continuous, global radio satellite system.					
<b>17. Key Words</b> Risk, Safety, Natural Resources, Measurement				<b>18. Distribution Statement</b>	
<b>19. Security Classification (of this report)</b> Unclassified.		<b>20. Security Classification (of this page)</b> Unclassified.		<b>21. No. of Pages</b> 20	<b>22. Price</b> N/A

## SI\* (MODERN METRIC) CONVERSION FACTORS

APPROXIMATE CONVERSIONS TO SI UNITS				
Symbol	When You Know	Multiply By	To Find	Symbol
<b>LENGTH</b>				
in	inches	25.4	millimeters	mm
ft	feet	0.305	meters	m
yd	yards	0.914	meters	m
mi	miles	1.61	kilometers	km
<b>AREA</b>				
in <sup>2</sup>	square inches	645.2	square millimeters	mm <sup>2</sup>
ft <sup>2</sup>	square feet	0.093	square meters	m <sup>2</sup>
yd <sup>2</sup>	square yard	0.836	square meters	m <sup>2</sup>
ac	acres	0.405	hectares	ha
mi <sup>2</sup>	square miles	2.59	square kilometers	km <sup>2</sup>
<b>VOLUME</b>				
fl oz	fluid ounces	29.57	milliliters	mL
gal	gallons	3.785	liters	L
ft <sup>3</sup>	cubic feet	0.028	cubic meters	m <sup>3</sup>
yd <sup>3</sup>	cubic yards	0.765	cubic meters	m <sup>3</sup>
NOTE: volumes greater than 1000 L shall be shown in m <sup>3</sup>				
<b>MASS</b>				
oz	ounces	28.35	grams	g
lb	pounds	0.454	kilograms	kg
T	short tons (2000 lb)	0.907	megagrams (or "metric ton")	Mg (or "t")
<b>TEMPERATURE (exact degrees)</b>				
°F	Fahrenheit	5 (F-32)/9 or (F-32)/1.8	Celsius	°C
<b>ILLUMINATION</b>				
fc	foot-candles	10.76	lux	lx
fl	foot-Lamberts	3.426	candela/m <sup>2</sup>	cd/m <sup>2</sup>
<b>FORCE and PRESSURE or STRESS</b>				
lbf	poundforce	4.45	newtons	N
lbf/in <sup>2</sup>	poundforce per square inch	6.89	kilopascals	kPa
APPROXIMATE CONVERSIONS FROM SI UNITS				
Symbol	When You Know	Multiply By	To Find	Symbol
<b>LENGTH</b>				
mm	millimeters	0.039	inches	in
m	meters	3.28	feet	ft
m	meters	1.09	yards	yd
km	kilometers	0.621	miles	mi
<b>AREA</b>				
mm <sup>2</sup>	square millimeters	0.0016	square inches	in <sup>2</sup>
m <sup>2</sup>	square meters	10.764	square feet	ft <sup>2</sup>
m <sup>2</sup>	square meters	1.195	square yards	yd <sup>2</sup>
ha	hectares	2.47	acres	ac
km <sup>2</sup>	square kilometers	0.386	square miles	mi <sup>2</sup>
<b>VOLUME</b>				
mL	milliliters	0.034	fluid ounces	fl oz
L	liters	0.264	gallons	gal
m <sup>3</sup>	cubic meters	35.314	cubic feet	ft <sup>3</sup>
m <sup>3</sup>	cubic meters	1.307	cubic yards	yd <sup>3</sup>
<b>MASS</b>				
g	grams	0.035	ounces	oz
kg	kilograms	2.202	pounds	lb
Mg (or "t")	megagrams (or "metric ton")	1.103	short tons (2000 lb)	T
<b>TEMPERATURE (exact degrees)</b>				
°C	Celsius	1.8C+32	Fahrenheit	°F
<b>ILLUMINATION</b>				
lx	lux	0.0929	foot-candles	fc
cd/m <sup>2</sup>	candela/m <sup>2</sup>	0.2919	foot-Lamberts	fl
<b>FORCE and PRESSURE or STRESS</b>				
N	newtons	0.225	poundforce	lbf
kPa	kilopascals	0.145	poundforce per square inch	lbf/in <sup>2</sup>
<small>*SI is the symbol for the International System of Units. Appropriate rounding should be made to comply with Section 4 of ASTM E380. (Revised March 2003)</small>				

## TABLE OF CONTENTS

List of Abbreviations .....	vii
Acknowledgments.....	viii
Executive Summary .....	ix
CHAPTER 1.INTRODUCTION .....	1
1.1. Problem Statement.....	1
1.2. Relevant Literature.....	2
CHAPTER 2.RESULTS AND NEXT STEPS .....	3
2.1. Research Tasks and Results .....	3
2.1.1. Conduct an Experiment of GNSS-R-Based Water Level and Wave Height Monitoring.....	3
2.1.2. Use GNSS-R to Measure Coastal Water Levels and Significant Wave Heights .....	3
2.1.3. Develop a Framework for Using GNSS-R Extracted Wave Heights and Water Levels to Assess Erosion Risk.....	7
2.2. Future Research .....	7
CHAPTER 3.REFERENCES .....	9

## LIST OF FIGURES

**Figure 1-1:** Coastal erosion threatening roads and coastal infrastructure. Left) Washaway Beach in Washington, red line was shoreline in 1990, image is from 2017. Middle) Gleneden beach in Oregon, example of cliff erosion that could also influence coastal roadways. Right) Port Heiden in Alaska was disconnected because of road failure in 2017..... 1

**Figure 1-2:** Schematic drawing of GNSS-based tide gage (taken from Kim and Park, 2019). ..... 2

**Figure 2-1:** Experimental set-up for GNSS-R measurement validation at the USACE Field Research Facility Pier in Duck, North Carolina.....3

**Figure 2-2:** Time series of water levels derived by the GNSS-R-based tide gauge, together with water levels from the tide gauge and the SWH from the buoy (from Kim et al., 2021b). .....5

**Figure 2-3:** Time series of the inverse CLR (black line) derived by the GNSS-R-based tide gauge, together with the SWH measured by the buoy (blue line) (taken from Kim et al., 2021b). .....6

**Figure 2-4:** Correlation between the inverse CLR from the GNSS-R-based tide gauge and the SWH from the buoy (taken from Kim et al., 2021b).....7

## **LIST OF ABBREVIATIONS**

CLR: Conditional logistic regression

GNSS: Global Navigation Satellite System

GNSS-R: Global Navigation Satellite System-Reflectometry

PacTrans: Pacific Northwest Transportation Consortium

SNR: Signal to noise

SWH: Significant wave height

## **ACKNOWLEDGMENTS**

We thank the U.S. Army Corps of Engineers Field Research Facility for helping us to deploy the GNSS antenna at the end of its research pier in Duck, North Carolina.

## EXECUTIVE SUMMARY

USDOT Region 10 includes three states that have extensive lengths of coastal roads (Oregon, Washington, and Alaska). In each state, long stretches of oceanfront roads are the only way to move goods and people between coastal cities and inland population centers, which makes their potential vulnerability critical. In each of Oregon, Washington, and Alaska, coastal erosion due to high water levels and high waves is a known hazard. Roads perched on top of coastal bluffs are at risk because of undercutting from combined high water levels and waves (Olsen et al. 2009), and roads near sea-level on open coasts are at risk because of changing shorelines.

Our objective was to develop a new technique to assess the hazard level of coastal erosion hotspots on existing and planned coastal roadways by continuously monitoring coastal water levels and wave heights with a new remote sensing technique that incorporates the land-based Global Navigation Satellite System (GNSS). The proposed technique will measure nearshore water levels and wave heights using land-based and easily mobilized GNSS, which is an all-weather, continuous, global radio satellite system. GNSS is a remote sensing technique. It is easy to install and maintain, and it is economical for departments of transportation with coastal roadways to buy with relatively low budgets (an antenna receiver is ~\$3000). GNSS can continuously monitor conditions during storms without being in destructive sea-states (like tide gages and coastal buoys) and without depending on optical clarity (like cameras). Additionally, the proposed method generates water level observations with respect to the geodetic datum, which is tied to the land survey datum, so there is no need to convert between datums as with other monitoring techniques.



## CHAPTER 1. INTRODUCTION

### 1.1. Problem Statement

USDOT Region 10 includes three states that have extensive lengths of coastal roads (Oregon, Washington, and Alaska). In each state, long stretches of oceanfront roads are the only way to move goods and people between coastal cities and inland population centers, which makes their potential vulnerability critical. In each of Oregon, Washington, and Alaska, coastal erosion due to high water levels and high waves is a known hazard. Roads perched on top of coastal bluffs are at risk because of undercutting from combined high water levels and waves (Olsen et al. 2009), and roads near sea-level on open coasts are at risk because of changing shorelines (figure 1-1).



**Figure 1-1:** Coastal erosion threatening roads and coastal infrastructure. Left) Washaway Beach in Washington, red line was shoreline in 1990, image is from 2017. Middle) Gleneden beach in Oregon, example of cliff erosion that could also influence coastal roadways. Right) Port Heiden in Alaska was disconnected because of road failure in 2017.

**Our objective was to develop a new technique to assess the hazard level of coastal erosion hotspots on existing and planned coastal roadways by continuously monitoring coastal water levels and wave heights with a new remote sensing technique that incorporates the land-based Global Navigation Satellite System (GNSS).** The proposed technique will measure nearshore water levels and wave heights using the land-based and easily mobilized GNSS, which is an all-weather, continuous, global radio satellite system. The GNSS is a remote sensing technique. It is easy to install and maintain, and it is economical for departments of transportation (DOTs) with coastal roadways to buy with relatively low budgets (an antenna receiver is ~\$3000). The GNSS can continuously monitor conditions during storms without being in destructive sea-states (like tide gages and coastal buoys) and without depending on optical clarity (like cameras). Additionally, the proposed method generates water level

observations with respect to the geodetic datum, which is tied to the land survey datum, so there is no need to convert between datums as with other monitoring techniques.

## 1.2. Relevant Literature

The GNSS, akin to the Global Positioning System (GPS), uses satellites to measure an accurate three-dimensional position of an antenna on a receiver. Unlike the typical method of GNSS positioning, which collects radio signals from GNSS satellites only directly to a receiver, this technique, referred to as GNSS-Reflectometry (GNSS-R), utilizes signals that have bounce off nearby objects before reaching the receiver, referred to as multipath signals. Figure 1-2 illustrates the concept of water level observations measured with GNSS multipath signals. The phase delay can be converted to the vertical distance from the water surface to the GNSS antenna, which is fixed on the ground. By continuously computing this vertical distance in time, the water level variation can be obtained as a time series. The feasibility of GNSS-R-based water level monitoring has been proved by a number of studies (e.g., Martin-Neira, 1997; Löfgren et al., 2011; Larson et al., 2013; Löfgren and Haas, 2014; Kim and Park, 2019), but the near real-time observation method using advanced GNSS has been only recently investigated by principal investigator Park. In addition, it should be emphasized that this technique measures sea levels with respect to the International Terrestrial Reference Frame (ITRF) (Löfgren and Haas, 2014; Kim and Park, 2019), which allows the water levels to be output be in a coordinate system consistent with that for land.

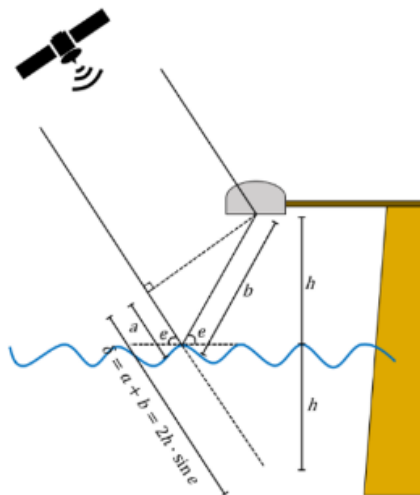


**Figure 1-2:** Schematic drawing of GNSS-based tide gage (taken from Kim and Park, 2019).

## CHAPTER 2. RESULTS AND NEXT STEPS

### 2.1. Research Tasks and Results

#### 2.1.1. *Conduct an Experiment of GNSS-R-Based Water Level and Wave Height Monitoring*

We deployed a GNSS-R antenna for nearly one year at the U.S. Army Corps of Engineers Field Research Facility in Duck, North Carolina. The site was chosen because the facility has a long pier where we were able to deploy the antenna over the water on a high pole for a long period of time, with power and Internet available for receiving data and connecting to the instrument remotely. Additionally, at the Army Corps facility there were continuous and trusted water level and significant wave height data streams that we could compare to the GNSS-R extracted measurements (<http://www.frf.usace.army.mil/>). Although the field site was not in USDOT Region 10, the findings are broadly applicable.

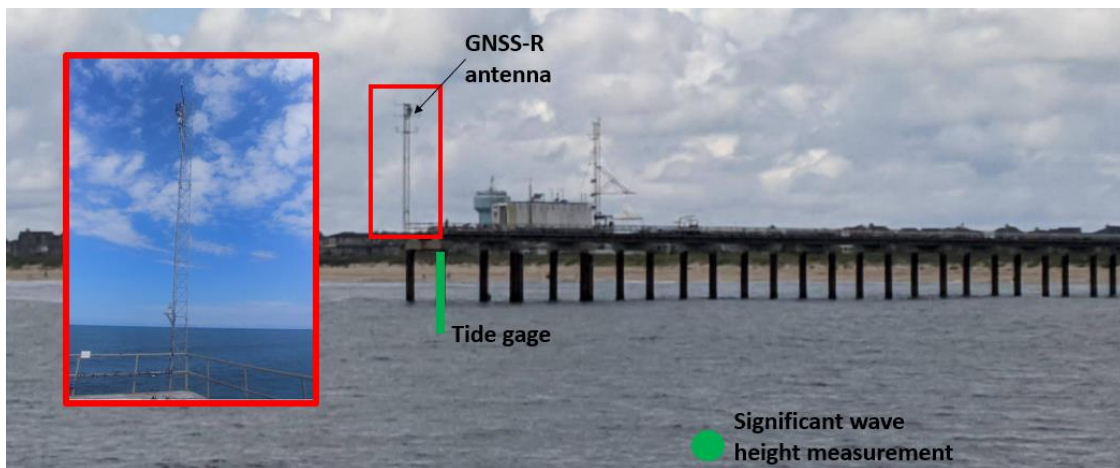


**Figure 2-1:** Experimental set-up for GNSS-R measurement validation at the USACE Field Research Facility Pier in Duck, North Carolina.

#### 2.1.2. *Use GNSS-R to Measure Coastal Water Levels and Significant Wave Heights*

GNSS-R measures water levels by analyzing oscillations in the signal to noise ratio (SNR) of GNSS signals reflected from the water surface. In the SNR data, the impact of the signal reflection represents the oscillation. The phase of these SNR oscillations,  $\theta$ , can be indicated on the basis of the geometric relationship between the satellite, the GNSS antenna, and the reflector (see figure 2-1).

$$\theta = \frac{2\pi}{\lambda} \delta = \frac{4\pi}{\lambda} h \sin e$$

where  $\lambda$  is the wave length of the GNSS signals,  $e$  is the satellite elevation angle, and  $h$  is the GNSS antenna height above the reflecting surface.  $\delta$  indicates the signal path delay caused by the reflection. Then, by taking a derivative of the phase with respect to the sine of the satellite elevation angle, the linear relationship between the frequency of the SNR oscillations,  $f$ , and the antenna height from the ocean surface can be derived.

$$f = \frac{2h}{\lambda}$$

Consequently, the antenna height over the water surface can be directly converted from the frequency of the SNR oscillations. The frequency of the oscillations can be determined by extracting the most dominant frequency through spectral analysis.

Figure 2-2 shows the time series of water levels derived from the experiment conducted in Duck, North Carolina, during December 4 through 31, 2020. Note that the GNSS unit experienced random power outages during the trial, which are indicated by gray shades in the plot. In general, the water level measurements between the tide gauge and the GNSS-R showed good agreement, except during a few days indicated in red boxes. Notably, large significant wave heights (SWH) were observed by the nearby wave buoy during that time period. One reason for the disagreement may be the distortion of reflected signals when the waves were very high.

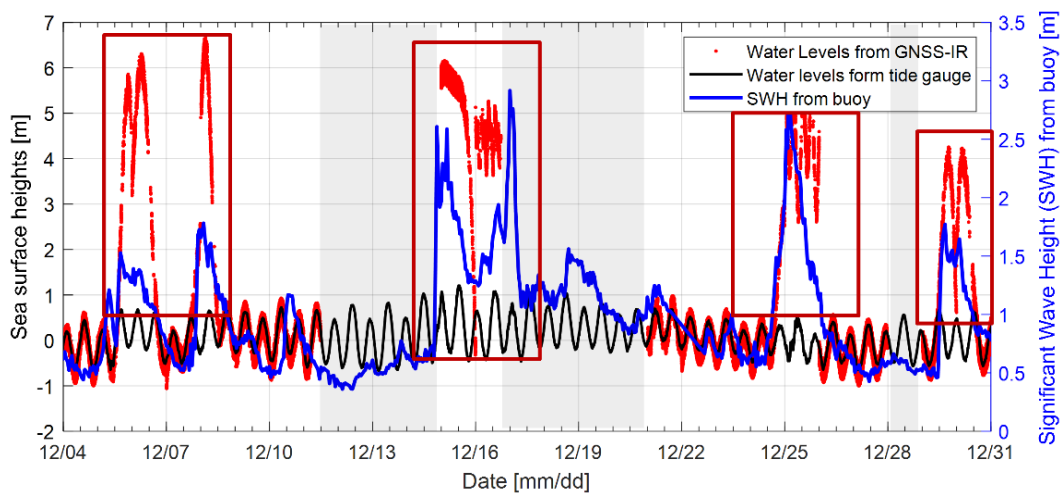


**Figure 2-2:** Time series of water levels derived by the GNSS-R-based tide gauge, together with water levels from the tide gauge and the SWH from the buoy (from Kim et al., 2021b).

The presence of high waves resulted in the distortion of the return signal, making it difficult to detect one dominant frequency. That was because some spectra of signals were reflected by the highest wave crests, and the rest of them gradually propagated into the wave troughs, resulting in reflections over several wave surfaces. That is, the higher waves generated the greatest distortions in the reflected signals, which resulted in multiple indistinctive frequencies in the spectral domain. Accordingly, this signal distortion made it difficult to determine the water level; however, it could be used as a tool to measure characteristics of wave height, such as SWH. To utilize the signal distortion for monitoring SWH, we used a numerical indicator, conditional logistic regression (CLR).

$$CLR = P_{\text{domi}} \frac{1}{\frac{1}{N-1} \sum_{i=1}^{N-1} P_{\text{rest},i}}$$

where  $P_{\text{domi}}$  and  $P_{\text{rest}}$  are the power of the peak marked as dominant and the other remaining peaks, respectively;  $N$  is the number of the peaks identified in the spectral domain. CLR was firstly introduced by Kim et al. (2019, 2021a) to assess the impact of a coastal event on water level determinations. CLR indicates the superiority of the dominant peak, representing the height of the reflecting surface with respect to the other remaining peaks in the spectral domain of the SNR signal. This means that CLR basically can serve as an effective parameter to indicate the coherence of the frequency generated by the ocean surface, and the degree of the coherence that varies with the presence and severity of the waves.

To monitor SWH with the GNSS-R-based tide gauge, we observed the CLR and compared it with the SWH observed by the nearby wave buoy in Duck, North Carolina, during December 4 through 31, 2020. As the CLR had an inverse relationship with the roughness of the reflecting surface, the inverse CLR was computed, which is shown as a black line in figure 2.3. Overall, the inverse CLR showed a pattern similar to that of the SWH measured by the buoy. As the SWH increased, the inverse CLR also increased, and conversely, when the SWH decreased, the inverse CLR also decreased. However, poor performance was also detected during certain time windows around the 16th and 22nd of December (red boxes in the figure). One possibility is the low quality of the collected GNSS data, given that significant data gaps existed on those dates.

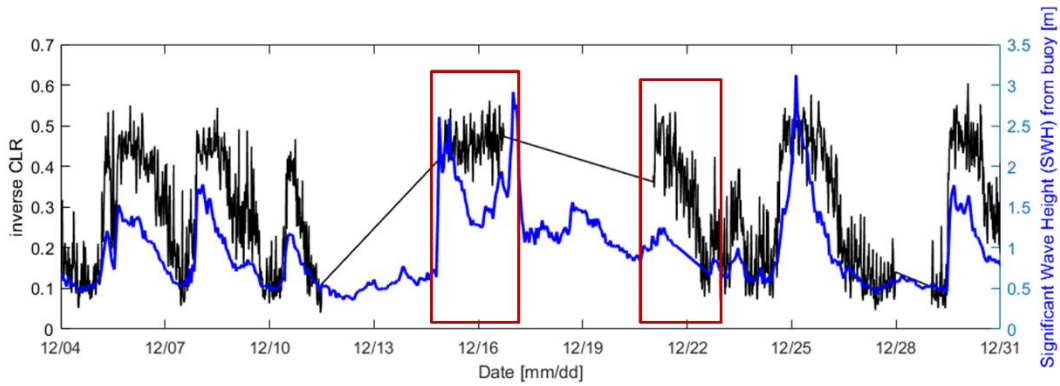


**Figure 2.3:** Time series of the inverse CLR (black line) derived by the GNSS-R-based tide gauge, together with the SWH measured by the buoy (blue line) (taken from Kim et al., 2021b).

In addition, we numerically analyzed the consistency between the inverse CRL from the GNSS-R and the SWH from the buoy (figure 2.4). The correlation coefficient between the two was 0.81, which can be considered a strong correlation. In particular, when the wave height was lower than 1.5 m, better agreement, 0.88, was confirmed. The results showed that the proposed approach is feasible for observing SWH, and it can be a complementary tool for monitoring SWH.

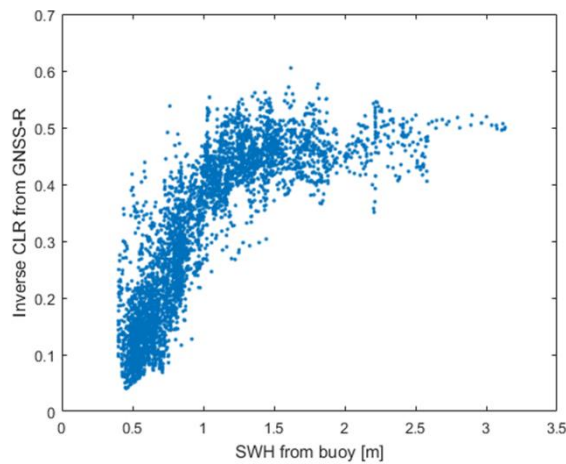


**Figure 2.4:** Correlation between the inverse CLR from the GNSS-R-based tide gauge and the SWH from the buoy (taken from Kim et al., 2021b).

Note that this section summarizes a conference paper presented at IEEE GNSS+R 2021, and more details about the methodologies and experimental results can be found in the paper by Kim et al. (2021b).

### *2.1.3. Develop a Framework for Using GNSS-R Extracted Wave Heights and Water Levels to Assess Erosion Risk*

To assess the vulnerability of coastal infrastructure to erosion, the following must be considered:

- substrate material (sand, rock shores, coastal cliffs)
- beach/berm width, slope, and volume in front of infrastructure
- dune/cliff/berm crest height
- beach orientation
- the total water level elevation
- wave power
- the impact hours of waves at a given water level (how long the water level remains high while wave heights are high).

With this information we can assess how vulnerable a given piece of infrastructure or proposed infrastructure may be to a coastal storm. The next step to developing a predictor for any given USDOT site would be to create a probabilistic framework based on simple analytical expressions that would be fed by measurements of total water levels and significant wave heights from the GNSS-R. The framework would predict the current or future vulnerability of infrastructure based on the set of inputs and relationships listed above (Beuzen et al., 2019). Beuzen et al. (2019) presented a Bayesian network framework for erosion risk with the listed input metrics. If the USDOT is interested in using wave heights and water levels measured with GNSS-R to assess the erosion potential of coastlines near DOT managed roadways, then the Bayesian network could be adapted with existing analytical formulations for dune erosion and cliff erosion by using the GNSS-R measured wave heights and water levels from existing antennas deployed by the coastline or from a new temporary antenna deployed near the coast during a season of storm events. These types of measurements could help a DOT assess whether a particular coastline was vulnerable to erosion. The measurements could also be used as real-time monitoring of already vulnerable DOT assets.

## 2.2. Future Research

The techniques developed in this work have led to a new project granted to principal investigator Park to implement the use of GNSS-R for monitoring water levels and potentially wave heights in remote areas in Alaska where reliable water level measurements are scarce. This

project will adapt GNSS as a new operational water level measurement tool, referred to as the GNSS Water Level Observation System (GWOS), which will improve existing coastal water level monitoring capabilities. During that project, an operational water level monitoring GNSS-R methodology will be developed. Also, we will characterize the site-dependent parameters of the GNSS-R for the east, west, and south coasts of the continental U.S. and Alaska to optimize the GWOS. The project will produce a standalone executable software package for producing water level measurements from GNSS-R data.

### CHAPTER 3. REFERENCES

- AOOS, Coastal and nearshore water level observations in Alaska: Challenges, Assets, Gaps, and Next Steps, June 2016, [http://aoos.org/wp-content/uploads/2011/05/2016\\_Alaska\\_Water\\_Level\\_Observations\\_v1-0.pdf](http://aoos.org/wp-content/uploads/2011/05/2016_Alaska_Water_Level_Observations_v1-0.pdf)
- Beuzen, T., Harley, M.D., Splinter, K.D. and Turner, I.L., 2019. Controls of variability in berm and dune storm erosion. *Journal of Geophysical Research: Earth Surface*, 124(11), pp.2647-2665.
- Kim S.K. and J. Park (2019), Monitoring Sea Level Change in the arctic using GNSS-Reflectometry, Proceedings in International Technical Meeting (ITM) 2019 - Institute of Navigation, 28-31 January 2019, Reston, Virginia.
- Kim, S.K., Lee, E., Park, J. and Shin, S. (2021a), Feasibility Analysis of GNSS-Reflectometry for Monitoring Coastal Hazards. *Remote Sens*, Vol 13, No. 5, pp. 976.
- Kim, S.K., Park, J., Shin, S., Lee, E. (2019), Feasibility Study of GNSS-Reflectometry for Tsunami Analysis. Proceedings in *AGU Fall Meeting 2019*. San Francisco, CA.
- Kim, S.K., Park, J., Wengrove, M.E., Dickey, J.E. (2021b), Feasibility Study Of GNSS Interferometric Reflectometry (GNSS-IR) For Retrieving Significant Wave Height. Proceedings in *GNSS+R 2021*. Virtual Conference.
- Larson, K., J. Löfgren, and R. Haas (2013), Coastal sea level measurements using a single geodetic GPS receiver, *Advances in Space Research*, Vol. 51, No. 8, pp. 1301-1310, 2013.
- Löfgren, J., Haas, R., and Johansson, J. (2011), Monitoring coastal sea level using reflected GNSS signals," *Advances in Space Research*, Vol. 47, No. 2, pp. 213-220.
- Löfgren, J.S. and Haas (2014), Sea level measurements using multi-frequency GPS and GLONASS observations, *R. EURASIP J. Adv. Signal Process.* 2014: 50. <https://doi.org/10.1186/1687-6180-2014-50>.
- Martin-Neira, M. (1993), A Passive Reflectometry and Interferometry System (PARIS): Application to Ocean Altimetry," *ESA Journal*, Vol. 17, pp. 331-355.
- Olsen, M. J., Johnstone, E., Driscoll, N., Ashford, S. A., & Kuester, F. (2009). Terrestrial laser scanning of extended cliff sections in dynamic environments: Parameter analysis. *Journal of Surveying Engineering*, 135(4), 161-169.

